Title

Engineered Cell-Secreted Extracellular Matrix Modulates Cell Spheroid Mechanosensing and Amplifies Their Response to Inductive Cues for the Formation of Mineralized Tissues

Permalink

https://escholarship.org/uc/item/7f84q0c2

Journal

Advanced Healthcare Materials, 11(10)

ISSN

2192-2640

Authors

Gonzalez-Fernandez, Tomas
Tenorio, Alejandro J
Saiz, Augustine M
et al.

Publication Date

2022-05-01

DOI

10.1002/adhm.202102337

Peer reviewed

Engineered Cell-Secreted Extracellular Matrix Modulates Cell Spheroid Mechanosensing and Amplifies Their Response to Inductive Cues for the Formation of Mineralized Tissues

Tomas Gonzalez-Fernandez, Alejandro J. Tenorio, Augustine M. Saiz Jr, and J. Kent Leach*

The clinical translation of mesenchymal stromal cell (MSC)-based therapies remains challenging due to rapid cell death and poor control over cell behavior. Compared to monodisperse cells, the aggregation of MSCs into spheroids increases their tissue-forming potential by promoting cell–cell interactions. However, MSCs initially lack engagement with an endogenous extracellular matrix (ECM) when formed into spheroids. Previously the instructive nature of an engineered, cell-secreted ECM is demonstrated to promote survival and differentiation of adherent MSCs. Herein, it is hypothesized that the incorporation of this cell-secreted ECM during spheroid aggregation would enhance MSC osteogenic potential by promoting cell–matrix and cell–cell interactions. ECM-loaded spheroids contained higher collagen and glycosaminoglycan content, and MSCs exhibited increased mechanosensitivity to ECM through Yes-associated protein (YAP) activation via integrin $\alpha 2\beta 1$ binding. ECM-loaded spheroids sustained greater MSC viability and proliferation and are more responsive to soluble cues for lineage-specific differentiation than spheroids without ECM or loaded with collagen. The encapsulation of ECM-loaded spheroids in instructive alginate gels resulted in spheroid fusion and enhanced osteogenic differentiation. These results highlight the clinical potential of ECM-loaded spheroids as building blocks for the repair of musculoskeletal tissues.

1. Introduction

Cell-based approaches for bone regeneration are under investigation as an alternative to autologous bone grafts and recombinant proteins for treatment of large bone deficits. Among various cell populations under consideration, mesenchymal stromal cells (MSCs) are a central focus due to their multipotency in vitro, a potent secretome that signals the endogenous healing program, and

a safety profile confirmed through numerous clinical trials. Clinical evidence supports the administration of MSCs to accelerate the repair of non-unions.[1] The established correlation between the number of viable transplanted MSCs and healing outcome motivates the need for novel approaches to maximize cell survival and engraftment, both of which remain a significant challenge for cell-based approaches to bone tissue regeneration.[2]

Aggregation of MSCs into three-dimensional (3D) spheroids enhances cell survival, trophic factor secretion, and tissue-forming potential compared to monodisperse cells.[3,4] Despite their therapeutic advantages, MSC spheroids were unable to bridge segmental bone defects without supplemental administration of bone morphogenetic protein-2 (BMP-2),[5] hypoxic preconditioning,[6] or chondrogenic priming.[7] MSC spheroids are formed by promoting cell-cell contacts via cadherin binding,[8] yet cells within spheroids initially lack engagement with an endogenous extracellular matrix (ECM) that is only achieved over time.

The ECM is a heterogeneous network of proteins and polysaccharides that provides sites for adhesion, mechanical stiffness, and transduces physical and biological signals to influence cell behavior.[9,10] Cell-secreted ECM produced in vitro is a promising approach to capture the complexity of the native ECM with reduced variability, along with the capacity to tune matrix composition through control of the culture microenvironment.[11] We previously described an MSC-secreted ECM composed of 278 distinct proteins, of which collagens make up ≈24% of total protein, with collagen types I, V, VI and VII being the most abundant.[12] Additionally, we demonstrated that cells engaging this MSC-secreted ECM, either in culture or on 3D macroporous scaffolds, exhibited increased osteogenic differentiation, maintained their osteogenic phenotype upon induction, and enhanced survival.[12–14] Thus, cell-secreted ECM is a naturally-derived platform to effectively improve the efficacy of cell-based approaches for tissue formation.

Given the prior success of spheroids and cell-secreted ECM to individually enhance the efficacy of MSCs, we hypothesized that the formation of MSC spheroids loaded with cell-secreted

T. Gonzalez-Fernandez, A. M. Saiz Jr, J. K. Leach
Department of Orthopaedic Surgery
UC Davis Health
Sacramento, CA 95817, USA
E-mail: jkleach@ucdavis.edu
A. J. Tenorio, J. K. Leach
Department of Biomedical Engineering
University of California, Davis
Davis, CA 95616, USA

The ORCID identification number(s) for the author(s) of this article can be found under https://doi.org/10.1002/adhm.202102337

DOI: 10.1002/adhm.202102337

ADVANCED
SCIENCE NEWS
www.advancedsciencenews.com

ADVANCED
HEALTHCARE
MATERIALS
www.advhealthmat.de

ECM would provide a platform to enhance MSC viability and differentiation potential through accelerating integrin engagement. As spheroids are formed by favoring cohesion to other cells over adhesion and engagement with the ECM, these studies were designed to explore the effect of loading spheroids with ECM at the time of aggregation. We evaluated the influence of ECM mass on cell survival and cell signaling. We further tested the response of MSC spheroids to inductive cues in vitro before encapsulation in instructive alginate hydrogels for the production of clinically relevant mineralized tissues. These results demonstrate the promise of activating cell-matrix signaling in conjunction with the benefits of spheroid formation.

2. Results

2.1. ECM Influences the Spheroid Physical and Biochemical Microenvironment

Cell-secreted ECM was incorporated into MSC spheroids at increasing masses (0, 1, 2.5, 5, or 7.5 µg ECM/spheroid). Spheroid diameter increased with increasing ECM mass (367.7 ± 36.4 µm for 0 µg, 398.2 ± 31.3 µm for 1 µg, 489.7 ± 54.5 µm for 2.5 µg, 566.7 ± 68.1 µm for 5 µg, and 590 ± 63.6 µm for 7.5 µg of ECM) (**Figure 1**A,F). Cells were more localized at the periphery for spheroids loaded with 1 µg ECM, while we observed cells distributed homogeneously throughout the spheroid when incorporating higher ECM masses (Figure 1B). There were no significant differences in DNA content among all groups (Figure 1G). MSCs in ECM-loaded spheroids exhibited more prominently stretched actin fibers (Figure 1C), larger cell area (Figure S2A, Supporting Information) and larger, more elongated nuclei (Figure S2B–D, Supporting Information). Collagen and GAG content increased with increasing masses of ECM (Figure 1D,E,H,I), confirming the manipulation of spheroid biochemical composition due to the efficient incorporation of exogenous collagen and GAG into the spheroids. Spheroid diameter, collagen, and GAG content were not significantly different between spheroids loaded with 5 and 7.5 µg ECM ($p = 0.9$ for spheroid diameter, $p < 0.9$ for GAG content, and $p = 0.6$ for collagen content), suggesting a plateau in ECM incorporation efficiency (Figure 1H,I).

The mechanical properties of ECM-loaded spheroids were measured to determine changes in the cellular microenvironment due to ECM incorporation. After formation, the Young's modulus of spheroids loaded with either 2.5, 5, or 7.5 µg of ECM was significantly higher ($p < 0.023$ for 2.5 µg ECM and $p < 0.001$ for 5 and 7.5 µg ECM) than the modulus of spheroids without ECM (**Figure 2**A,B, Supporting Information).

### 2.2. ECM Regulates Integrin Expression and MSC Mechanosensing

As cell adhesion is controlled by integrin binding to specific ligands within the ECM, we next assessed the expression of integrin subunits in MSCs aggregated into ECM-loaded spheroids. We analyzed the expression of integrin subunits $\alpha2$, $\alpha5$, and $\beta1$ two days after spheroid formation, as these integrins were upregulated in MSCs on ECM-coated plates.[12] We detected significantly greater expression of integrin subunits $\alpha2$ (*ITGA2*) and $\beta1$

(*ITGB1*) in spheroids loaded with 5 and 7.5 µg of ECM compared to unloaded spheroids ($p = 0.047$ and $p = 0.024$ for integrin subunit $\alpha2$, and $p = 0.0013$ and $p = 0.0002$ for integrin subunit $\beta1$) (**Figure 3**A,C), while integrin $\alpha5$ (*ITGA5*) was increased only in spheroids loaded with 5 µg ECM ($p = 0.035$) (Figure 3B). We measured the expression of N-cadherin (*CDH2*) to confirm that cell–cell contacts were not impaired in ECM-loaded spheroids. We observed similar *CDH2* expression among the groups, with significantly higher expression in spheroids loaded with 5 µg ECM compared to spheroids loaded with 1 µg ECM ($p = 0.029$) (Figure 3D). We then explored the impact of increased integrin expression on YAP gene expression and translocation into the nucleus, as YAP is a key transcription factor for MSCs to sense changes in ECM stiffness and adhesion proteins.[15] We observed significant increases in *YAP1* expression in spheroids loaded with 5 and 7.5 µg ECM compared to unloaded spheroids ($p = 0.013$ and $p = 0.0036$, respectively) (Figure 3E). Immunostaining of YAP revealed more intense staining with increasing ECM content (Figure 3G), confirming changes in gene expression. In addition, the translocation of YAP into the cell nucleus 1 day after spheroid formation was greater as ECM mass increased (Figure 3F,G).

Previous studies have shown that both substrate stiffness and adhesion ligand density mediate cytoskeletal tension and YAP activation.[16,17] To investigate the relationship between ECM ligand density achieved by ECM loading and YAP expression, integrin $\alpha2\beta1$ was blocked by supplementation of the culture media with an $\alpha2\beta1$ antibody. Media supplementation with the blocking antibody did not impair spheroid cell viability (*data not shown*). After 3 days of spheroid formation, gene expression of *YAP1* and *CDH2* was significantly lower in ECM-loaded spheroids cultured in $\alpha2\beta1$ blocking conditions ($p = 0.0001$ and $p = 0.034$, respectively) compared to expression in spheroids without ECM (**Figure 4**A–C). In addition, imaging of the actin cytoskeleton and YAP confirmed a more disorganized, loose actin cytoskeleton and less YAP staining in ECM-loaded spheroids when $\alpha2\beta1$ was abrogated (Figure 4D).
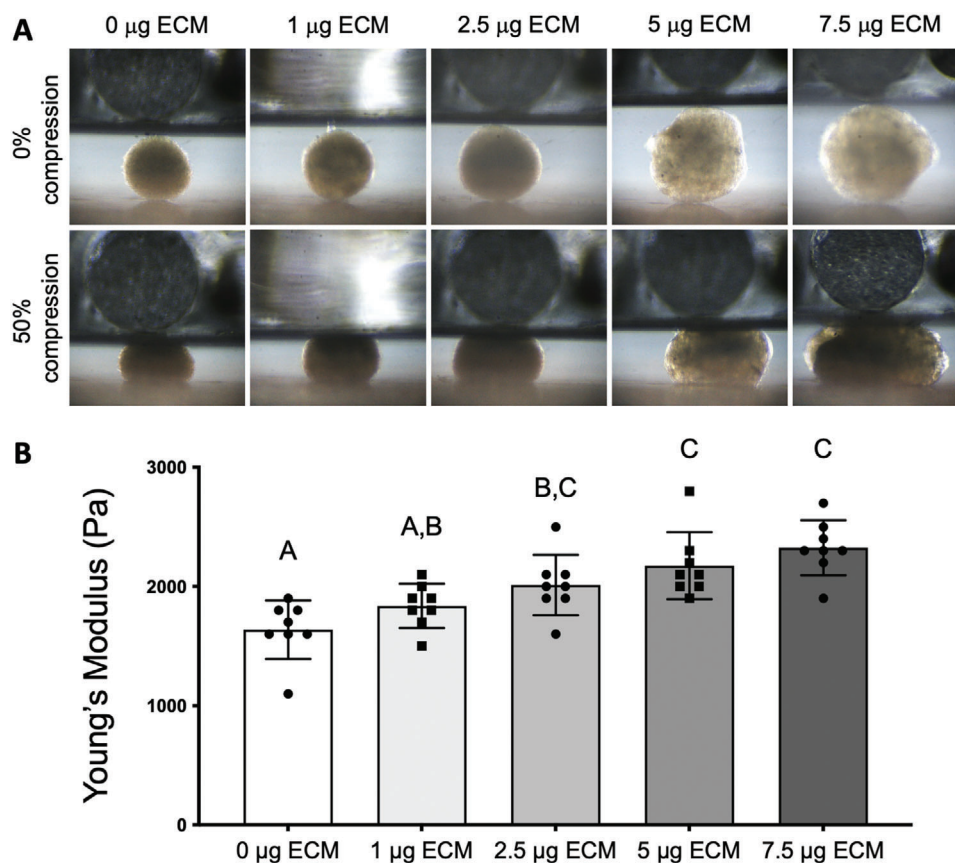
2.3. ECM Enhances MSC Survival and Proliferation

To assess the effects of ECM on MSC viability in vitro, we analyzed cell viability, metabolic activity, proliferation, and apoptosis of spheroids loaded with increasing masses of ECM over 7 days (Figure S3, Supporting Information). Live/dead staining of ECM-loaded spheroids confirmed that spheroids contained viable cells in all groups and time points (Figure S3A, Supporting Information). We observed significantly higher metabolic activity in spheroids containing 7.5 µg ECM compared to unloaded spheroids at all time points ($p = 0.0009$ at day 1, $p < 0.0001$ at days 3 and 7), while spheroids loaded with 5 µg ECM had significantly higher metabolic activity compared to spheroids with no ECM or 1 µg ECM at days 3 and 7 ($p = 0.018$ at day 3 and $p < 0.0001$ at day 7) (Figure S3B, Supporting Information). We detected higher DNA content in spheroids loaded with 2.5, 5, and 7.5 µg ECM compared to 0 and 1 µg of ECM at day 7 (Figure S3C, Supporting Information). Moreover, spheroids loaded with 5 and 7.5 µg ECM contained significantly more DNA at day 7 compared to day 1, suggesting increased MSC proliferation in ECM-loaded spheroids (Figure S3C, Supporting Information). We observed
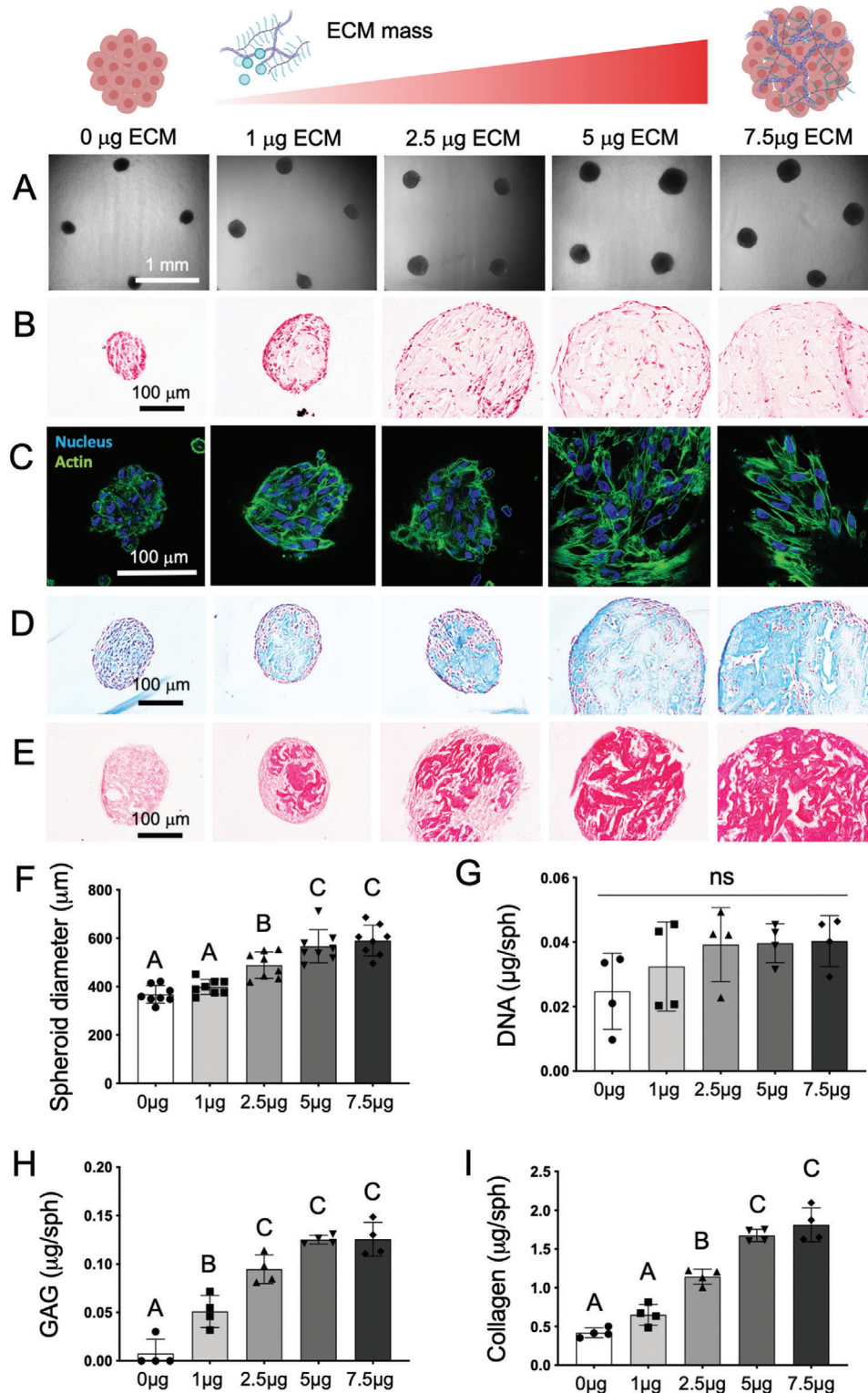
Figure 1. Spheroid morphology, biochemical composition, and cellular tension is influenced by ECM incorporation. A) Brightfield microscopy of ECM-loaded spheroids after production. B) Representative H&E staining of spheroids after formation. C) Fluorescent imaging of actin cytoskeleton (green) and cell nucleus (blue) of MSCs in ECM-loaded spheroids 48 h after formation. Histological examination of D) GAG and E) collagen content through Alcian blue/fast red and picrosirius red staining, respectively. F) Quantification of spheroid diameter ($n = 8$). Biochemical quantification of G) DNA content, H) GAG content, and I) collagen content of the ECM-loaded spheroids after production ($n = 4$).

**ADVANCED
SCIENCE NEWS**

www.advancedsciencenews.com

**ADVANCED
HEALTHCARE
MATERIALS**

www.advhealthmat.de

Figure 2. ECM-loaded spheroids exhibit higher Young's modulus with increasing ECM mass. A) Representative images of ECM-loaded spheroids before compression and after compression to 50% deformation. B) Elastic modulus of ECM-loaded spheroids ($n = 8$).
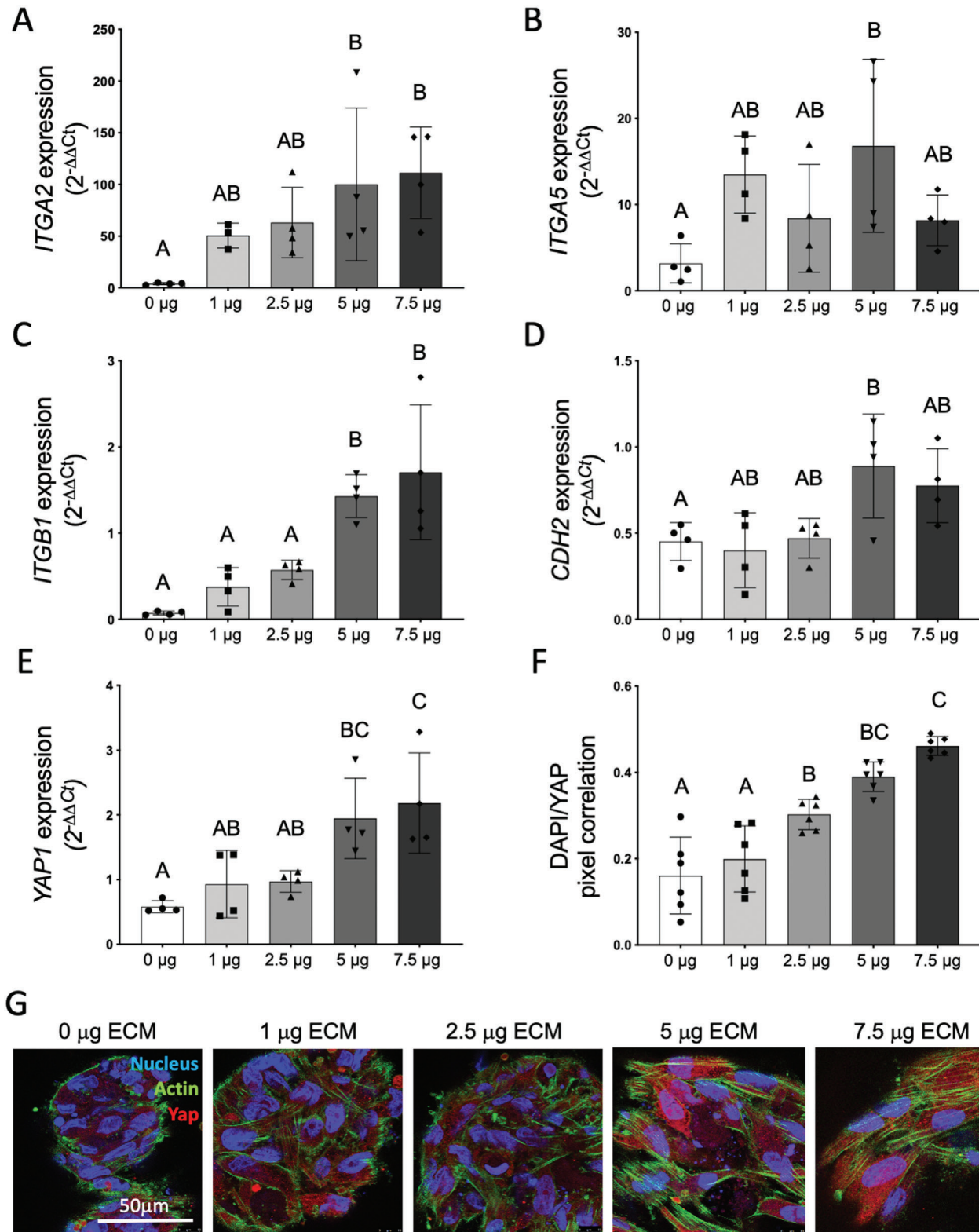
higher caspase 3/7 activity in spheroids without ECM compared to spheroids loaded with 2.5, 5, and 7.5 μg of ECM at every time point (Figure S3D, Supporting Information).

### 2.4. MSC Differentiation is Increased in ECM-Loaded Spheroids

To assess the effect of ECM incorporation on the chondrogenic and osteogenic potential of MSCs, spheroids with or without ECM were differentiated in either chondrogenic (CM) or osteogenic media (OM). 5 μg ECM/spheroid was selected due to plateaus in efficiency of ECM incorporation (Figure 1), integrin subunits $\alpha 2$ and $\beta 1$ and YAP expression (Figure 3), and cell viability at day 7 (Figure S4, Supporting Information). Due to the role of integrin $\alpha 2\beta 1$ in MSC cytoskeletal conformation and YAP expression (Figure 4) and the abundance of collagen type I in the cell-secreted ECM,[12] spheroids loaded with 5 μg of collagen were included as a control (**Figure 5**A). After 10 days of differentiation, we assessed the gene expression of aggrecan (*ACAN*) and collagen type II (*COL2A*) as chondrogenic markers and *RUNX2* and osteocalcin (*BGLAP*) as osteogenic markers. The expression of collagen type X (*COL10A1*) was analyzed in both differentiation conditions as a marker of endochondral ossification. MSCs in ECM-loaded spheroids exhibited significantly higher expression of *ACAN* when cultured in chondrogenic media and *BGLAP* when cultured in osteogenic media ($p = 0.0245$ and $p = 0.0001$, re-

spectively) (Figure 5B,E). *COL10A1* expression was significantly higher in collagen and ECM-loaded spheroids in chondrogenic media ($p = 0.044$ and $p = 0.0038$) and in ECM-loaded spheroids when cultured in osteogenic media ($p = 0.0089$) compared to spheroids without ECM (Figure 5F,G).

After 21 days of differentiation, ECM-loaded spheroids exhibited significantly higher quantities of DNA, collagen, and GAG content in either growth (GM), chondrogenic (CM), or osteogenic (OM) culture conditions compared to control and collagen-loaded spheroids (more than 4-fold increase across all lineages, $p < 0.0001$ in GM for DNA, GAG and collagen, $p < 0.05$ in CM, $p < 0.00001$ in OM) (**Figure 6**A–C). Although no statistical differences in calcium levels were observed among the groups in osteogenic media (Figure 6C), ECM-loaded spheroids exhibited early foci of mineralization by day 11 with a highly mineralized matrix at day 21 that confirmed effective osteogenic induction (Figure 6I). In contrast, calcium deposition in spheroids with 0 μg ECM or 5 μg collagen was evident on the spheroid periphery and was not distributed through the internal matrix, as observed by an increase in debris around these spheroids (Figure S4A, Supporting Information), decrease in spheroid diameter (Figure S4B, Supporting Information), and lack of calcified matrix in the spheroid interior (Figure S4C, Supporting Information). Despite significantly higher collagen content at day 2 after spheroid formation (Figure 6C), confirming effective ECM incorporation, spheroids loaded with type I collagen exhibited similar

**ADVANCED
SCIENCE NEWS**

www.advancedsciencenews.com

**ADVANCED
HEALTHCARE
MATERIALS**

www.advhealthmat.de

Figure 3. ECM incorporation into MSC spheroids enhances integrin expression and cell mechanosensing. Gene expression of integrin subunits A) $\alpha2$ (*ITGA2*); B) $\alpha5$ (*ITGA5*); C) $\beta1$ (*ITGB1*); D) N-cadherin (*CDH2*); and E) YAP (*YAP1*) 2 days after spheroid formation ($n = 4$). F) Quantification of nuclear YAP by DAPI/YAP pixel correlation ($n = 6$). G) Immunofluorescent detection of YAP (red), actin cytoskeleton (green) and cell nucleus (blue) in MSCs on spheroids loaded with increasing concentrations of ECM after 1 day of spheroid formation.
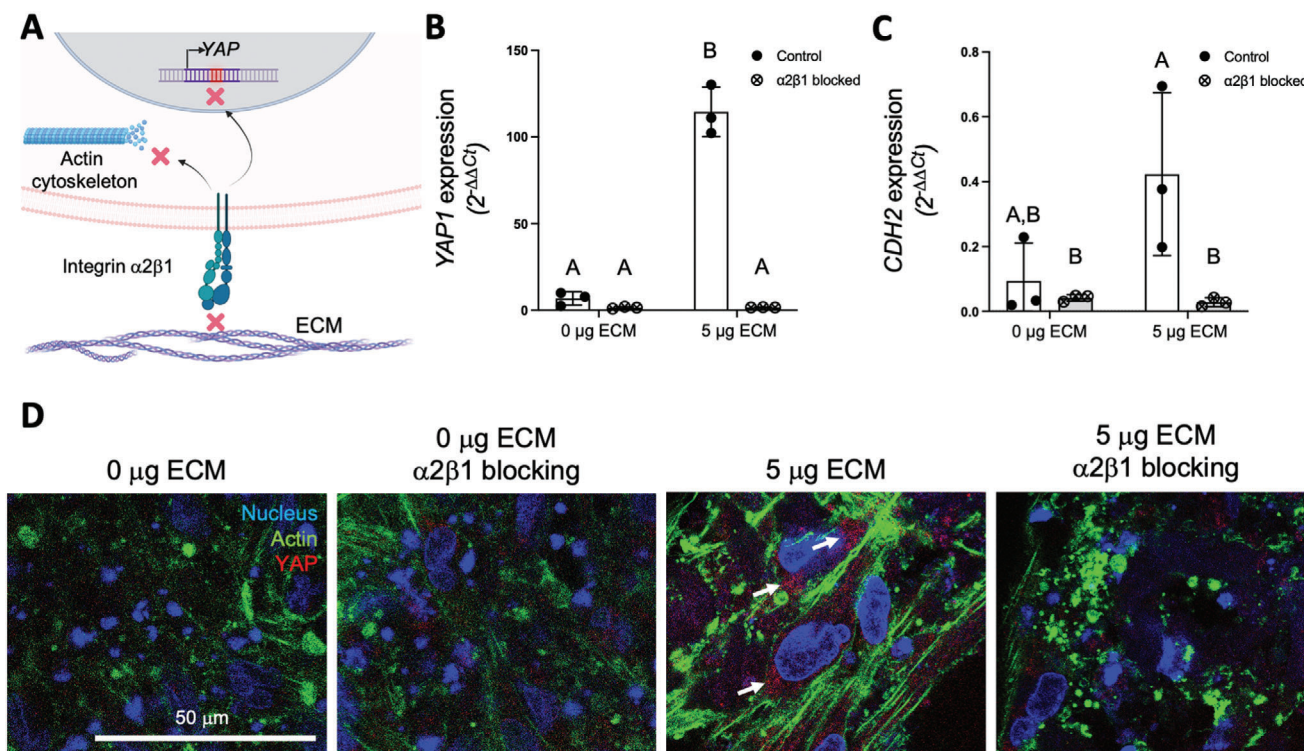
Figure 4. Blocking of integrin $\alpha2\beta1$ adhesion regulates YAP and N-cadherin expression and the cytoskeletal tension of MSCs in ECM-loaded spheroids. A) Schematic of the effects of integrin $\alpha2\beta1$ blocking on YAP expression and actin cytoskeleton. Gene expression analysis of B) YAP (*YAP1*) and C) N-cadherin (*CDH2*) in spheroids loaded with 0 μg and 5 μg of ECM after 3 days of culture in standard media or media supplemented with $\alpha2\beta1$ antibody (*n* = 3). D) Representative immunofluorescence of YAP (red), actin cytoskeleton (green) and cell nuclei (blue) in MSCs on spheroids loaded with 0 μg and 5 μg of ECM after 3 days of culture in standard media or media supplemented with $\alpha2\beta1$ antibody. White arrows denote areas of positive YAP staining.

diameters (Figure S4B, Supporting Information) and biochemical indices of differentiation as control spheroids (0 μg ECM) for all media after 21 days (Figure 6B–D), confirming that the observed response to ECM-loaded spheroids was not solely due to the presence of collagen type I in the incorporated ECM.

2.5. ECM-Loaded Spheroids in Instructive Hydrogels as Building Blocks for Mineralized Tissues

Having established the efficacy of ECM-loaded spheroids, we then tested the osteogenic potential of ECM-loaded spheroids entrapped in clinically relevant alginate hydrogels, which are widely studied for cell transplantation. Control spheroids (0 μg ECM) or spheroids with 5 μg ECM were encapsulated in alginate hydrogels functionalized with either low (DS2) or high (DS10) concentrations of RGD adhesive ligands (**Figure 7**A). After 21 days in OM, we observed viable cells that sprouted from the spheroids into the alginate matrix in all groups suggesting promotion of spheroid fusion (Figure 7B). DNA content in gels containing ECM-loaded spheroids was significantly greater at day 21 compared to gels containing control spheroids (Figure 7G). Additionally, gels containing ECM-loaded spheroids contained significantly more DNA content at day 21 compared to day 1, suggesting the maintenance of cell viability and enhanced cell proliferation. Histological analysis of the spheroid-laden hydrogels

revealed intense staining for collagen at day 21, specifically for collagen types I and X, markers of endochondral ossification, in ECM-loaded spheroids compared to control spheroids (Figure 7C–E). Biochemical quantification of collagen and GAG content confirmed higher GAG and collagen deposition in the ECM spheroids independent of RGD content at day 21 compared to control spheroids (Figure 7H,I). However, collagen content at day 21 was significantly higher compared to day 1 only in the ECM-loaded spheroids encapsulated in high RGD alginate ($p = 0.0053$). We observed calcified spheroids in all groups after 21 days of osteogenic differentiation (Figure 7F), the quantity of which was not significantly different among groups (Figure 7J).

3. Discussion

The clinical effectiveness of cell-based approaches for musculoskeletal repair has been underwhelming to date, particularly when assessing their direct contribution to bone formation. While it is widely agreed that MSCs play an important role in tissue repair through secretion of trophic factors that signal neighboring host cells,[18] these cells die quickly upon implantation and have limited ability to undergo differentiation in situ. Transplanted cells die through anoikis following separation from their native ECM, as occurs upon trypsinization during culture expansion. MSC spheroids exhibit improved survival and therapeutic advantages over monodisperse cells due to increased
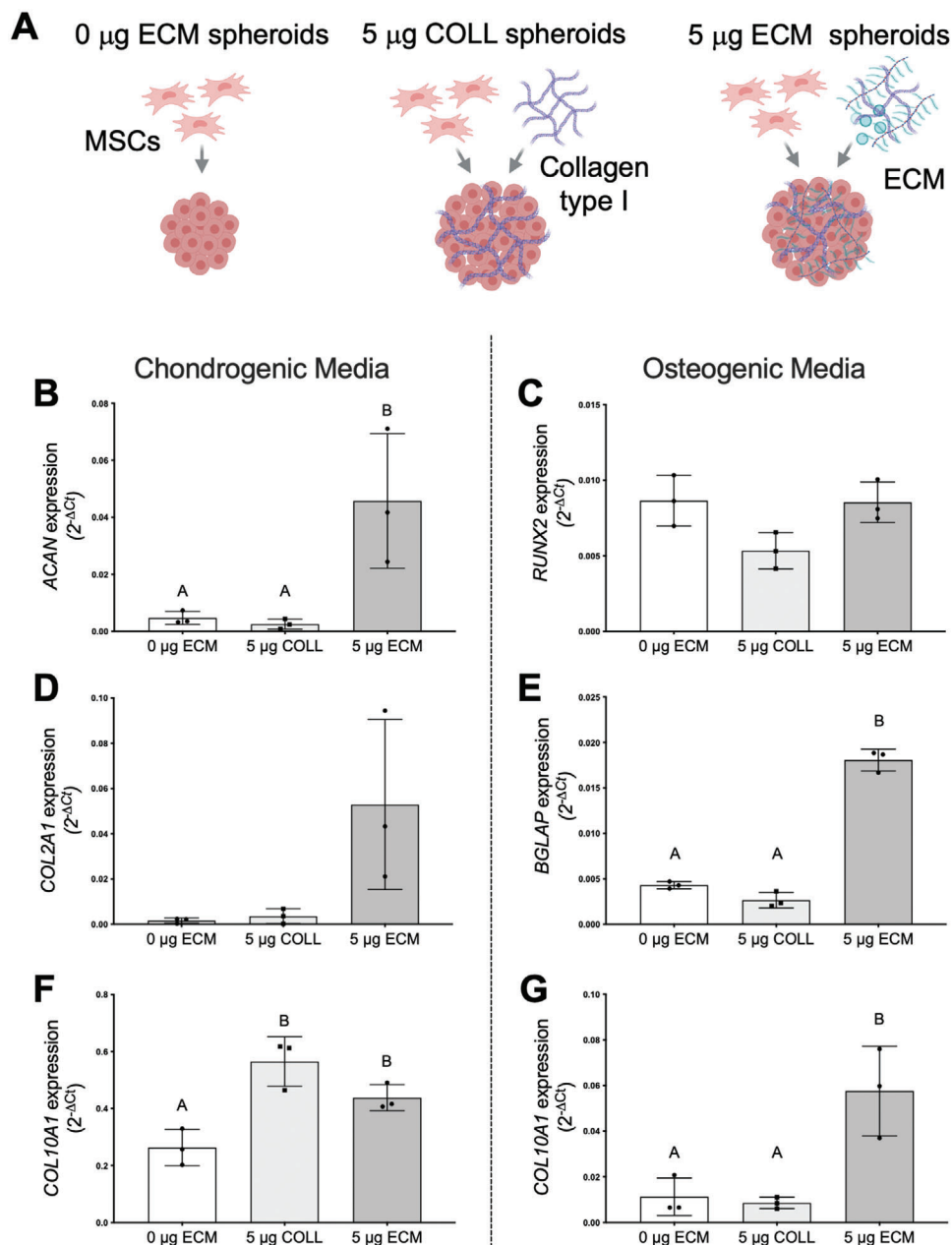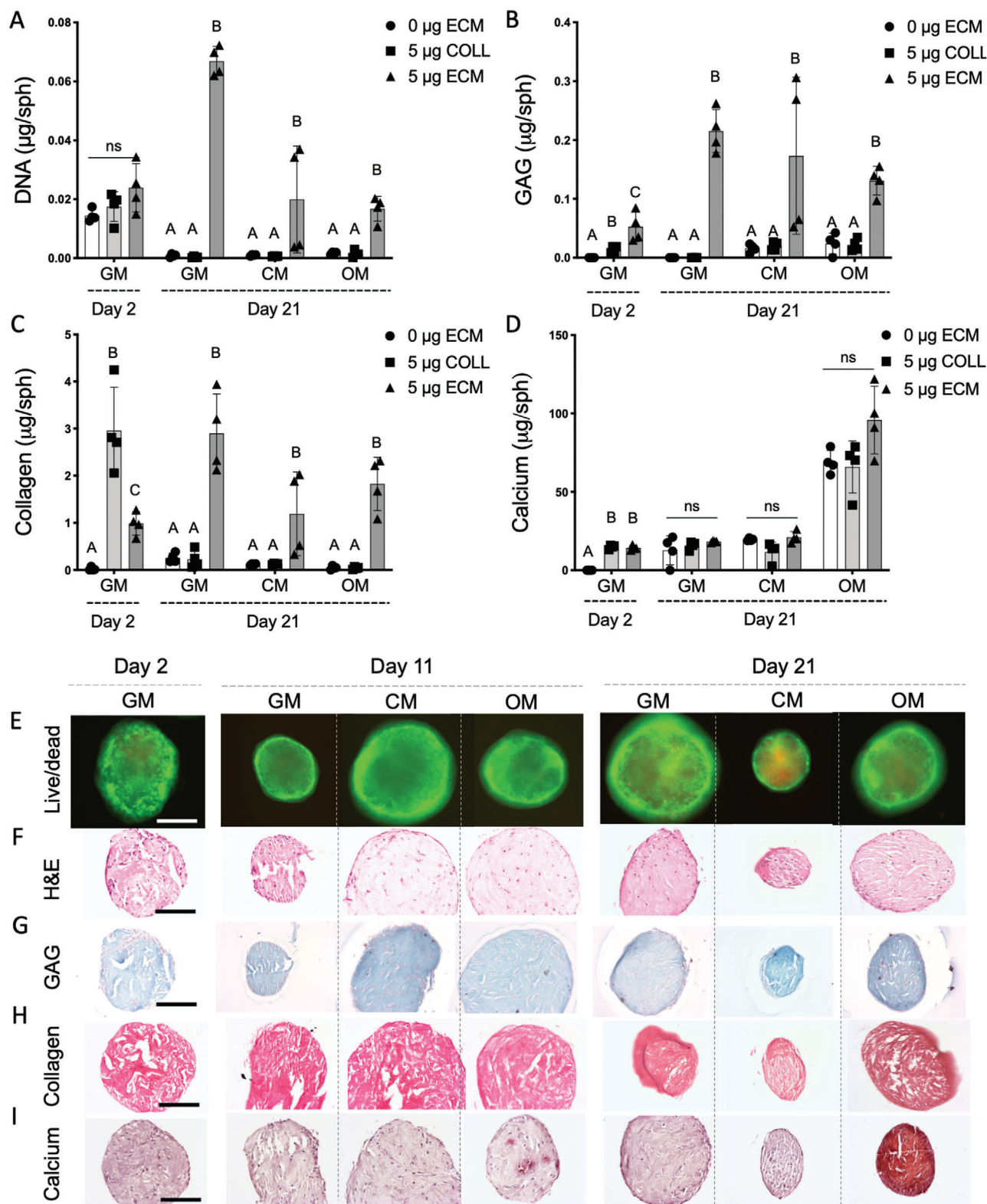
Figure 5. ECM incorporation into MSC spheroids enhances the expression of chondrogenic and osteogenic differentiation markers. A) Schematic describing experimental groups. B) Gene expression of aggrecan (*ACAN*); C) *RUNX2*; D) collagen type II (*COL2A1*); E) osteocalcin (*BGLAP*); and F,G) collagen type X (*COL10A1*) in spheroids without ECM and spheroids loaded with 5 µg of collagen or ECM in chondrogenic or osteogenic conditions ($n = 3$).

cell–cell interactions, yet these aggregates initially lack substantial ECM to promote integrin–ligand interactions that modulate MSC function.[10,19] The lack of ECM engagement may be a contributing factor for why spheroids are unable to repair large bone deficits without adjuvant inductive cues or other preconditioning approaches.[6,5b] In the current study, ECM incorporation into MSC spheroids increased integrin expression and YAP nuclear translocation within MSCs, which correlated with increased viability, proliferation, and multilineage potential in vitro. The encapsulation of ECM-loaded spheroids in instructive alginate hy-

drogels led to spheroid fusion and the production of osteogenic tissues, highlighting the potential of ECM-loaded spheroids for their use in the repair of damaged bone.

Cell-secreted ECM offers similar advantages to tissue-derived ECM, such as adhesion ligand complexity, ease of remodeling, and cytokine interaction while overcoming its limitations by offering improved tunability, availability, and reduced batch-to-batch variability. We selected an MSC-secreted ECM previously identified in our lab to maximize osteogenic differentiation of MSCs[11–13,20,21] for incorporation into spheroids and to propel

ADVANCED
SCIENCE NEWS

www.advancedsciencenews.com

ADVANCED
HEALTHCARE
MATERIALS

www.advhealthmat.de

Figure 6. MSC spheroids containing cell-secreted ECM exhibit increased multilineage potential. Biochemical quantification of A) DNA; B) GAG; C) collagen; and D) calcium content in spheroids loaded with no ECM (0 µg ECM), 5 µg of collagen type 1 (5 µg COLL), or 5 µg of ECM (5 µg ECM) at day 2 and 21 after formation and cultured in growth (GM), chondrogenic (CM), or osteogenic (OM) media (*n* = 4). E) Representative live/dead imaging; F) H&E; G) GAG; H) collagen; and I) Alizarin red staining of spheroids loaded with 5 µg ECM at days 2, 11, and 21 after formation and cultured in GM, CM, and OM. Scale bar = 100 µm for all images.
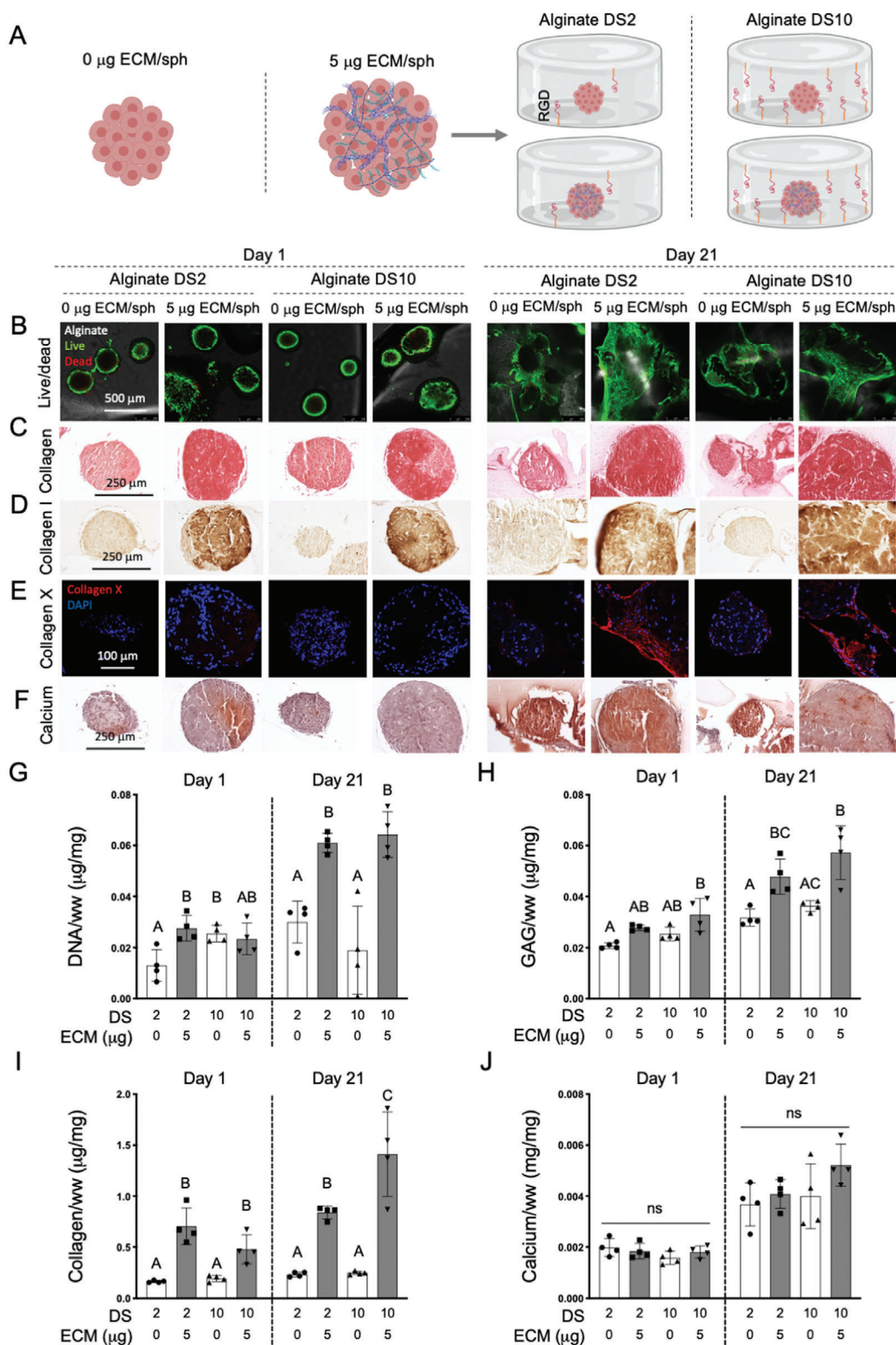
Figure 7. Osteogenic potential of ECM-loaded spheroids in bio-instructive alginate hydrogels. A) ECM-loaded (5 µg ECM) or control spheroids (0 µg ECM) were encapsulated in alginate gels functionalized with low (DS2) or high (DS10) concentration of RGD. B) Representative live/dead confocal imaging of alginate hydrogels with MSC spheroids containing no ECM or 5 µg ECM at day 1 and 21 in OM. Histological and immunohistochemical analysis of C) collagen; D) collagen type I; E) collagen type X; and F) calcium of hydrogel-encapsulated spheroids at days 1 and 21 of osteogenic culture. Biochemical quantification of G) DNA; H) GAG; I) collagen; and J) calcium content of the spheroid-loaded alginate hydrogels after 1 and 21 days of osteogenic culture ($n = 4$). Scale bar = 500 µm for (A) and 250 µm for (B), (C), and (D).

ADVANCED
SCIENCE NEWS

www.advancedsciencenews.com

ADVANCED
HEALTHCARE
MATERIALS

www.advhealthmat.de

their therapeutic potential. We observed increases in collagen and GAG content with increasing mass of ECM, in agreement with previous results reporting that collagen and GAGs account for ≈24% and 5%, respectively, of MSC-derived ECMs.[12] We observed higher expression of integrin subunits $\alpha 2$ and $\beta 1$, components of integrin $\alpha 2\beta 1$ that MSCs require to bind to fibrillar collagen. We also observed increased MSC spreading and formation of actin stress fibers, revealing improved cell–substrate interactions in the ECM-loaded spheroids. These findings are in agreement with similar studies in which MSCs were seeded on 2D substrates coated with MSC-secreted ECM.[12] Despite the inclusion of ECM that enhances cell-ECM engagement, gene expression analysis of N-cadherin confirmed that cell-to-cell contact was not impaired in ECM-loaded spheroids. Thus, these results challenge the paradigm that spheroid formation must favor cell–cell contact and suppress cell–ECM interactions, providing an opportunity to better recapitulate the developmental process of cell condensation.[22] In addition, spheroid loading with ECM resulted in higher Young's modulus, highlighting the capacity of ECM enrichment to also modulate the spheroid mechanical microenvironment. The mechanical properties of cell spheroids depend on cellular cytoskeletal forces, cell–cell interactions, and the ECM.[23] Nanomechanical analysis of carcinoma cell spheroids identified stiffer areas which correlated to the presence of collagen fibrils,[24] and spheroid treatment with collagenase resulted in a decrease in stiffness,[25] confirming the fundamental role of ECM in modulating bulk spheroid stiffness.

MSC engagement with the surrounding ECM has downstream effects on various signaling pathways through the activation of Akt,[26] PI3K,[27] MAPK,[27] and YAP/TAZ,[15,17,28] among others, which have decisive implications in cell mechanosensing, survival, and MSC differentiation. YAP is a key regulator of cell response to the ECM, stability of the actin cytoskeleton, and cell tension.[29] We observed increased YAP expression and nuclear YAP as the mass of incorporated ECM increased. These results agree with previous reports establishing that increasing ligand density can induce nuclear YAP translocation regardless of the substrate mechanical properties, and blocking of $\alpha v\beta 3$, $\alpha 5$, and $\alpha 2\beta 1$ integrins impaired YAP nuclear translocation.[15,28,30] To confirm the role of integrin $\alpha 2\beta 1$ in cellular cytoskeletal conformation and YAP expression, this integrin was blocked, leading to a decrease in YAP and N-cadherin expression and a less tense actin cytoskeleton. Therefore, ECM incorporation into MSC spheroids is a promising method to activate cell signaling pathways that promote survival and differentiation.

Integrin binding, cytoskeletal tension, and YAP translocation mediate cell survival and differentiation.[15] We previously demonstrated that cell-secreted ECM enhanced MSC osteogenic differentiation in 2D through a2β1 integrin binding and the activation of the ERK1/2 pathway.[20] In this study, ECM-loaded spheroids in chondrogenic or osteogenic conditions achieved higher expression of aggrecan and osteocalcin, respectively, and higher DNA, collagen, and GAG content compared to spheroids with no ECM or collagen-loaded spheroids. Early calcification and mineralized foci were observed at day 11 in ECM-loaded spheroids in osteogenic conditions. Although the activation of the ERK1/2 pathway was not investigated in this study, early calcification in the ECM-loaded spheroids may be due to the synergistic effect of YAP activation and ERK1/2 signaling, leading to

enhanced MSC osteogenic differentiation.[28,31] By day 21 of osteogenic culture, we observed a calcified collagen- and GAG-rich matrix throughout ECM-loaded spheroids, whereas other groups secreted calcium to the spheroid periphery.

The presence of a highly mineralized matrix in ECM-loaded spheroids suggests that ECM incorporation facilitates the biomineralization process that is characterized by deposition of apatite crystals inside collagen fibrils and the formation of biomineralization foci through the action of non-collagenous proteins.[32] Non-collagenous proteins, GAGs, and other proteoglycans in the ECM[12,20] could have a role in matrix biomineralization, either by the direct binding of Ca^{2+} ions and control of crystal nucleation[33] or indirectly, by the entrapment of MSC-secreted proteins during osteogenesis that may initiate biomineralization.[32] GAGs may also bind growth factors such as BMP-2,[34] TGF-$\beta 1$,[35] and VEGF[36] via ionic interactions and synergize with cellular receptors to tune their biological action. The interaction of GAGs in the incorporated ECM with soluble growth factors in the differentiation media, such as TGF-$\beta 3$ and other cytokines secreted by the MSCs, could have an essential role for the observed increased chondrogenic and osteogenic differentiation of MSCs in ECM-loaded spheroids.

The encapsulation of spheroids within instructive biomaterials prior to implantation is an effective strategy to promote cell persistence and local engraftment,[37] preventing uncontrolled spheroid dissociation and maximizing MSC function and survival after transplantation.[4,38] Previously, the encapsulation of MSC spheroids in RGD-modified alginate hydrogels resulted in improved survival, angiogenic factor secretion, and osteogenesis compared to spheroids in unmodified alginate.[4] Compared to unmodified gels, RGD-modified gels facilitated spheroid fusion after 5 days of culture through the promotion of cell migration,[4] which demonstrates the utility of RGD-modified alginate as platform for spheroid fusion and the production of larger tissues. Furthermore, the osteogenic potential of MSC spheroids can be tailored through the concentration of RGD on the alginate matrix.[39] In previous studies, MSC spheroids entrapped in alginate gels with lower RGD concentration exhibited increased cell migration from the spheroid into the surrounding alginate, while restricted migration, achieved using unmodified alginate or alginate with a high RGD concentration, was associated with increased in vivo bone formation.[39] Although we observed significantly higher DNA, collagen, and GAG content in ECM-loaded spheroids in both low and high RGD hydrogels compared to control spheroids after 21 days of osteogenic culture, we did not appreciate differences in MSC migration or calcification between the groups. This discrepancy may be due to the prior use of osteogenically primed MSCs[39] versus non-induced cells in this work. Compared to unloaded spheroids, ECM-loaded spheroids encapsulated in alginate gels also stained positive for collagen type I and X, markers of endochondral ossification.[40] This is likely due to the synergy between the ECM in the spheroid and the RGD peptide in the alginate substrate. While the RGD peptide was key to promote cell migration and spheroid fusion, the ECM provided additional insoluble signals, such as those present in fibronectin, perlecan, and other GAGs, to guide the MSC phenotype toward endochondral ossification. This synergistic effect and the contributions of individual components of the ECM toward endochondral ossification will be explored in future studies.

**ADVANCED
SCIENCE NEWS**

www.advancedsciencenews.com

**ADVANCED
HEALTHCARE
MATERIALS**

www.advhealthmat.de

4. Conclusions

These data demonstrate that the incorporation of cell-secreted ECM into MSC spheroids is a promising approach for enhancing the therapeutic potential of spheroids. The addition of ECM to MSC spheroids increased mechanosensing, survival, and differentiation regardless of the desired lineage specification. These results have implications for improving the efficacy of autologous cell-based approaches to musculoskeletal repair using MSCs, a clinically relevant, safe, and readily accessible cell source.

5. Experimental Section

Cell Culture: Human bone marrow-derived MSCs (Lonza, Walkersville, MD) from a single donor (male, 22 years old, mycoplasma negative) were expanded until passage 3–4 in standard culture conditions (37 °C, 21% O_2, 5% CO_2) in growth media (GM) composed of minimum essential alpha medium (α-MEM; w/L-glutamine, w/o ribo/deoxyribonucleosides (Invitrogen, Carlsbad, CA)) supplemented with 10% fetal bovine serum (FBS; Atlanta Biologicals, Flowery Branch, GA) and 1% penicillin (10 000 U mL^{-1}) and streptomycin (10 mg mL^{-1}, Mediatech, Manassas, VA) (P/S). The trilineage potential of these cells was characterized to confirm their multipotency before use (Figure S1, Supporting Information).

MSC-Secreted ECM Production: Cell-secreted ECM was prepared as previously described.[13,14,20] After culture, monolayers were washed with phosphate buffered saline (PBS) and cells were lysed using a 0.5% Triton X-100 and 20×10^{-3} M ammonium hydroxide (NH_4OH) solution followed by DNase I (all from MilliporeSigma, St. Louis, MO) treatment (37 °C for 1 h) to remove 99.9% of DNA content from culture postdecellularization.[11] Decellularized ECM was washed 3× with PBS and mechanically dislodged from culture flasks using a cell scraper. Total protein within the collected ECM was quantified using a bicinchoninic acid (BCA) protein assay (Thermo Fisher, Rockford, IL). ECM solutions were frozen in 0.02 N acetic acid at −20°C until use. Before use, cell-secreted ECM was lyophilized for 24 h to form a powder that was then resolubilized in GM.

Spheroid Formation and Differentiation: MSCs were aggregated into spheroids using a microwell-based centrifugation method as described.[41] The micropatterned agarose molds contained 29 microwells for formation of 29 spheroids per well. Briefly, after trypsinization and filtering using a 41 µm filter, MSCs (4.35×10^5 cells mL^{-1}; 15000 cells per spheroid) were pipetted into stamp-micropatterned agarose molds inserted in 24 well plates and centrifuged at 500×*g* for 8 min. Plates were maintained statically in standard culture conditions in GM for 48 h to form spheroids. For ECM-loaded spheroids, the ECM suspension was mixed with filtered MSCs to produce a homogeneous mixture and then pipetted into the molds, centrifuged, and maintained statically for 48 h for cell aggregation. Collagen type I from rat tail (Corning, NY, USA) was used as a control.

For α2β1 integrin blocking studies, integrin α2β1 antibody (ab24697, Abcam) was dissolved in growth media at 5 µg mL^{-1} as previously described.[42] After cell seeding on agarose microwells and centrifugation, media was replaced by media containing α2β1 antibody and subsequently refreshed every 48 h.

For osteogenic and chondrogenic induction, MSC spheroids were maintained in either osteogenic (OM) or chondrogenic (CM) differentiation media. OM was composed of GM supplemented with 50×10^{-3} M ascorbate 2-phosphate, 10×10^{-3} M β-glycerophosphate, and 100×10^{-6} M dexamethasone (all from MilliporeSigma). CM was composed of chemically defined media consisting of Dulbecco's Modified Eagle Medium (DMEM, Invitrogen) supplemented with 1% penicillin (10 000 U mL^{-1}) and streptomycin (10 mg mL^{-1}, Mediatech), 100 mg mL^{-1} sodium pyruvate, 40 mg mL^{-1} L-proline, 50 mg mL^{-1} ascorbate 2-phosphate, 1.5 mg mL^{-1} BSA, 1× insulin–transferrin–selenium,

100×10^{-6} M dexamethasone (all from MilliporeSigma) and 10 ng mL^{-1} transforming growth factor β3 (PeproTech, Rocky Hill, NJ). Media was changed every 2–3 days.

Analysis of Biochemical Composition: Spheroids and hydrogels were collected and digested with papain (125 mg mL^{-1}, pH 6.5) in 0.1 M sodium acetate, 5×10^{-6} M L-cysteine HCl, and 0.05 M EDTA (all from MilliporeSigma) at 60 °C under constant rotation for 18 h. DNA and GAG content were quantified using the PicoGreen Quant-iT Assay Kit (Invitrogen) and the dimethyl methylene blue dye-binding (DMMB) assay, respectively. Total collagen content was determined by measuring hydroxyproline content using the dimethylaminobenzaldehyde and chloramine T assay, assuming a hydroxyproline to collagen ratio of 1:7.69.[43] Calcium content was determined using a Stanbio Calcium Liquid Reagent for Diagnostic Set (Thermo Fisher) after digestion in 1 M HCl at 60 °C for 72 h.

Analysis of Mechanical Properties: Spheroids were tested in a parallel-plate compression configuration using a CellScale MicroSquisher (CellScale, Ontario, Canada) and SquisherJoy software program. After spheroid formation, spheroids were collected and fixed in 4% paraformaldehyde (PFA) overnight at 4 °C and washed in PBS. After fixation, spheroids were placed in a PBS bath and compressed to 50% deformation over 30 s using a 0.5599 mm diameter stainless steel beam and a 6×6 mm platen. The force-displacement data obtained from the test were converted to stress/strain curves that were used to determine the Young's modulus in the linear portion of the curve as previously described.[44] Eight spheroids were analyzed per group.

Histological Characterization: Samples were collected and fixed in 4% PFA overnight at 4 °C and washed in PBS. Spheroids were encapsulated in Histogel (Thermo Fisher) to form 4×1 mm discs and then dehydrated in a graded series of ethanol baths and paraffin-embedded overnight. Each sample was sectioned at 7 µm thickness (RM2235 Manual Rotary Microtome) and affixed to microscope slides for subsequent staining. The sections were stained with hematoxylin and eosin (H&E), picrosirius red to assess collagen content, Alcian blue/fast red to stain sulfated glycosaminoglycans (GAG), and Alizarin red to assess calcification. Collagen type I (1:200; AB90395, Abcam, Cambridge, MA) and collagen type X (1:100; AB49945, Abcam) were detected using standard immunohistochemical and immunofluorescence techniques, respectively.

To visualize cell morphology and the actin cytoskeleton, spheroids were fixed overnight, washed twice with PBS, and permeabilized with 0.05% Triton-X 100 for 5 min at room temperature. The cell actin cytoskeleton was stained with Alexa Fluor 488 Phalloidin solution (Thermo Fisher; 1:40 in PBS), and cell nuclei were stained with DAPI (Thermo Fisher; 1:500 in PBS). Gels were imaged using a µ-Slide 8 Well (IBIDI, Planegg, Germany) through confocal microscopy (Leica TCS SP8, Wetzlar, Germany). Shape descriptors were analyzed using ImageJ with at least 4 separate images per group. YAP staining (1:100; sc-101199, Santa Cruz Biotechnology) was detected using a standard immunohistochemical technique. Analysis of YAP/nucleus colocalization was performed using CellProfiler (version 3.1.9) by correlation of staining DAPI/YAP pixels in 6 separate images per group.

Analysis of Cell Proliferation, Apoptosis, and Gene Expression: Spheroids were collected, washed with PBS, stained with live/dead assay per the manufacturer's protocol (Thermo Fisher), and fluorescent images were taken using confocal microscopy. For quantification of DNA levels and caspase 3/7 activity, constructs were collected, lysed in passive lysis buffer (Promega, Madison, WI), and sonicated. Total DNA content was evaluated using a PicoGreen Quant-iT DNA Assay Kit. Cell apoptosis was measured using a Caspase-Glo 3/7 assay (Promega, Madison, WI). Cell metabolic activity was evaluated through the alamarBlue assay per the manufacturer's protocol (Thermo Fisher).

For gene expression analysis, samples were collected in TRIzol (Invitrogen) for PCR analysis following the manufacturer's instructions. After RNA isolation, RNA was reverse transcribed with the QuantiTect Reverse Transcription kit (Qiagen, Valencia, CA) and qPCR was performed using Quantifast Probe PCR kit (Qiagen) on a QuantStudio5 system (Applied Biosystems). Primers and probes for housekeeping gene RPL13 (Hs00744303_s1), integrin subunits *ITGA2* (a$_2$, Hs00158127_m1), *ITGA5* (a$_5$, Hs01547673_m1) and *ITGB1* (b$_1$, HS01127536_m1), *YAP1* (YAP,

**ADVANCED
SCIENCE NEWS**

www.advancedsciencenews.com

**ADVANCED
HEALTHCARE
MATERIALS**

www.advhealthmat.de

Hs00902712_g1), *CDH2* (N-cadherin, Hs00983056_m1), *ACAN* (aggrecan, Hs00153936_m1), *COL2A1* (collagen type II, Hs00264051_m1), *BGLAP* (osteocalcin, Hs01587814_g1), *RUNX2* (Hs01047973_m1), and *COL10A1* (collagen type X, Hs00166657_m1) were purchased from Thermo Fisher. Amplification conditions were 95 °C for 3 min, followed by 45 cycles at 95 °C for 3 s and 60 °C for 30 s. Quantitative PCR results were normalized to *RPL13* transcript levels to yield ΔCt and/or to cells prior spheroid aggregation to yield $\Delta\Delta$Ct, and fold change in expression was calculated using $2^{-\Delta\Delta Ct}$.

Entrapment of Spheroids in RGD-Modified Alginate Hydrogels: Ultrapure VLVG sodium alginate (Pronova FMC BioPolymer, Norway) was covalently modified with Arg-Gly-Asp (RGD) peptide (Commonwealth Biotechnologies, Richmond, VA) using carbodiimide chemistry as reported.[4,45] The molar ratio of RGD to alginate was varied such that each alginate chain possessed a degree of substitution (DS) of either 2 or 10. Peptide conjugation was confirmed by nuclear magnetic resonance (NMR) and degree of substitution was assessed through the LavaPep Fluorescent Protein and Peptide Quantification Kit per the manufacturer's instructions (Gel Company, San Francisco, CA). The modified alginate was then lyophilized for one week and resuspended in PBS.

For entrapment, spheroids were mixed with the alginate solution to form a homogeneous 2% alginate-spheroid suspension (10×10^6 cells mL^{-1}) and pipetted into silicon molds. Hydrogels (6 mm diameter × 2 mm height) were formed by crosslinking with 100×10^{-3} M CaCl$_2$ (MilliporeSigma) for 10 min using a dialysis membrane.[46] After crosslinking, hydrogels were placed in growth or lineage-specific media and cultured in vitro under standard conditions for 21 days.

Statistical Analysis: All data represent a minimum of three independent experiments. Data are presented as means ± standard deviation unless otherwise stated. Statistical analysis utilized a one-way ANOVA with post-hoc Tukey test. $p < 0.05$ was considered significant. In each graph, data points with different letters are significantly different from one another. Lack of statistical significance between the groups is marked with "ns" and a line bridging non-significant groups.

Supporting Information

Supporting Information is available from the Wiley Online Library or from the author.

Conflict of Interest

The authors declare no conflict of interest.

Data Availability Statement

The data that support the findings of this study are available from the corresponding author upon reasonable request.

[1] a) K. Killington, R. Mafi, P. Mafi, W. S. Khan, *Curr. Stem Cell Res. Ther.* **2018**, *13*, 284; b) E. Gomez-Barrena, P. Rosset, D. Lozano, J. Stanovici, C. Ermthaller, F. Gerbhard, *Bone* **2015**, *70*, 93.

[2] a) E. M. Horwitz, D. J. Prockop, L. A. Fitzpatrick, W. W. Koo, P. L. Gordon, M. Neel, M. Sussman, P. Orchard, J. C. Marx, R. E. Pyeritz, M. K. Brenner, *Nat. Med.* **1999**, *5*, 309; b) P. Hernigou, A. Poignard, F. Beaujean, H. Rouard, *J. Bone Jt. Surg., Am. Vol.* **2005**, *87*, 1430.

[3] a) M. A. Gionet-Gonzales, J. K. Leach, *Biomed. Mater.* **2018**, *13*, 034109; b) P. R. Baraniak, T. C. McDevitt, *Cell Tissue Res.* **2012**, *347*, 701; c) Y. Yamaguchi, J. Ohno, A. Sato, H. Kido, T. Fukushima, *BMC Biotechnol.* **2014**, *14*, 105.

[4] S. S. Ho, K. C. Murphy, B. Y. Binder, C. B. Vissers, J. K. Leach, *Stem Cells Transl. Med.* **2016**, *5*, 773.

[5] a) S. S. Ho, N. L. Vollmer, M. I. Refaat, O. Jeon, E. Alsberg, M. A. Lee, J. K. Leach, *Adv. Healthcare Mater.* **2016**, *5*, 2501; b) A. B. Allen, J. A. Zimmermann, O. A. Burnsed, D. C. Yakubovich, H. Y. Stevens, Z. Gazit, T. C. McDevitt, R. E. Guldberg, *J. Mater. Chem. B* **2016**, *4*, 3594.

[6] S. S. Ho, B. P. Hung, N. Heyrani, M. A. Lee, J. K. Leach, *Stem Cells* **2018**, *36*, 1393.

[7] J. van der Stok, M. K. Koolen, H. Jahr, N. Kops, J. H. Waarsing, H. Weinans, O. P. van der Jagt, *Eur. Cells Mater.* **2014**, *27*, 137.

[8] a) M. W. Laschke, M. D. Menger, *Trends Biotechnol.* **2017**, *35*, 133; b) E. Fennema, N. Rivron, J. Rouwkema, C. van Blitterswijk, J. de Boer, *Trends Biotechnol.* **2013**, *31*, 108.

[9] K. H. Vining, D. J. Mooney, *Nat. Rev. Mol. Cell Biol.* **2017**, *18*, 728.

[10] U. Blache, M. M. Stevens, E. Gentleman, *Nat. Biomed. Eng.* **2020**, *4*, 357.

[11] M. L. Decaris, J. K. Leach, *Ann. Biomed. Eng.* **2011**, *39*, 1174.

[12] J. N. Harvestine, H. Orbay, J. Y. Chen, D. E. Sahar, J. K. Leach, *J. Mater. Chem. B* **2018**, *6*, 4104.

[13] A. I. Hoch, V. Mittal, D. Mitra, N. Vollmer, C. A. Zikry, J. K. Leach, *Biomaterials* **2016**, *74*, 178.

[14] J. N. Harvestine, T. Gonzalez-Fernandez, A. Sebastian, N. R. Hum, D. C. Genetos, G. G. Loots, J. K. Leach, *Sci. Adv.* **2020**, *6*, 2387.

[15] S. Dupont, L. Morsut, M. Aragona, E. Enzo, S. Giulitti, M. Cordenonsi, F. Zanconato, J. L. Digabel, M. Forcato, S. Bicciato, N. Elvassore, S. Piccolo, *Nature* **2011**, *474*, 179.

[16] C. Yang, M. W. Tibbitt, L. Basta, K. S. Anseth, *Nat. Mater.* **2014**, *13*, 645.

[17] S. Lee, A. E. Stanton, X. Tong, F. Yang, *Biomaterials* **2019**, *202*, 26.

[18] Y. Fu, L. Karbaat, L. Wu, J. Leijten, S. K. Both, M. Karperien, *Tissue Eng., Part B* **2017**, *23*, 515.

[19] F. Guilak, D. M. Cohen, B. T. Estes, J. M. Gimble, W. Liedtke, C. S. Chen, *Cell Stem Cell* **2009**, *5*, 17.

[20] M. L. Decaris, A. Mojadedi, A. Bhat, J. K. Leach, *Acta Biomater.* **2012**, *8*, 744.

[21] J. N. Harvestine, A. M. Saiz Jr, J. K. Leach, *Biomater. Sci.* **2019**, *7*, 2091.

[22] Y. W. Liu, B. Kuang, B. B. Rothrauff, R. S. Tuan, H. Lin, *Biomaterials* **2019**, *218*, 119336.

[23] Y. M. Efremov, I. M. Zurina, V. S. Presniakova, N. V. Kosheleva, D. V. Butnaru, A. A. Svistunov, Y. A. Rochev, P. S. Timashev, *Biophys. Rev.* **2021**, *13*, 541.

[24] V. Vyas, M. Solomon, G. G. M. D'Souza, B. D. Huey, *Cell Mol. Bioeng.* **2019**, *12*, 203.

[25] D. Jaiswal, N. Cowley, Z. Bian, G. Zheng, K. P. Claffey, K. Hoshino, *PLoS One* **2017**, *12*, e0188346.

[26] C. Popov, T. Radic, F. Haasters, W. C. Prall, A. Aszodi, D. Gullberg, M. Schieker, D. Docheva, *Cell Death Dis.* **2011**, *2*, e186.

[27] A. K. Kundu, C. B. Khatiwala, A. J. Putnam, *Tissue Eng., Part A* **2009**, *15*, 273.

[28] A. E. Stanton, X. Tong, F. Yang, *Acta Biomater.* **2019**, *96*, 310.

[29] G. Nardone, J. Oliver-De La Cruz, J. Vrbsky, C. Martini, J. Pribyl, P. Skladal, G. Pesl, G. Caluori, S. Pagliari, F. Martino, Z. Maceckova, M. Hajduch, A. Sanz-Garcia, N. M. Pugno, G. B. Stokin, G. Forte, *Nat. Commun.* **2017**, *8*, 15321.

[30] B. Zhao, X. Wei, W. Li, R. S. Udan, Q. Yang, J. Kim, J. Xie, T. Ikenoue, J. Yu, L. Li, P. Zheng, K. Ye, A. Chinnaiyan, G. Halder, Z. C. Lai, K. L. Guan, *Genes Dev.* **2007**, *21*, 2747.

[31] T. P. Driscoll, B. D. Cosgrove, S. J. Heo, Z. E. Shurden, R. L. Mauck, *Biophys. J.* **2015**, *108*, 2783.

[32] J. P. Gorski, *Front. Biosci. - Landmark* **2011**, *16*, 2598.

[33] J. L. Arias, A. Neira-Carrillo, J. I. Arias, C. Escobar, M. Bodero, M. David, M. S. Fernández, *J. Mater. Chem.* **2004**, *14*, 2154.

[34] V. Hintze, S. A. Samsonov, M. Anselmi, S. Moeller, J. Becher, M. Schnabelrauch, D. Scharnweber, M. T. Pisabarro, *Biomacromolecules* **2014**, *15*, 3083.

[35] L. Koehler, S. Samsonov, S. Rother, S. Vogel, S. Kohling, S. Moeller, M. Schnabelrauch, J. Rademann, U. Hempel, M. T. Pisabarro, D. Scharnweber, V. Hintze, *Sci. Rep.* **2017**, *7*, 1210.

[36] L. Koehler, G. Ruiz-Gomez, K. Balamurugan, S. Rother, J. Freyse, S. Moller, M. Schnabelrauch, S. Kohling, S. Djordjevic, D. Scharnweber, J. Rademann, M. T. Pisabarro, V. Hintze, *Sci. Rep.* **2019**, *9*, 18143.

[37] K. C. Murphy, S. Y. Fang, J. K. Leach, *Cell Tissue Res.* **2014**, *357*, 91.

[38] T. Gonzalez-Fernandez, P. Sikorski, J. K. Leach, *Acta Biomater.* **2019**, *96*, 20.

[39] S. S. Ho, A. T. Keown, B. Addison, J. K. Leach, *Biomacromolecules* **2017**, *18*, 4331.

[40] C. Scotti, B. Tonnarelli, A. Papadimitropoulos, A. Scherberich, S. Schaeren, A. Schauerte, J. Lopez-Rios, R. Zeller, A. Barbero, I. Martin, *Proc. Natl. Acad. Sci. U. S. A.* **2010**, *107*, 7251.

[41] T. Gonzalez-Fernandez, A. J. Tenorio, J. K. Leach, *3D Print. Addit. Manuf.* **2020**, *7*, 139.

[42] K. C. Murphy, A. I. Hoch, J. N. Harvestine, D. Zhou, J. K. Leach, *Stem Cells Transl. Med.* **2016**, *5*, 1229.

[43] N. Y. Ignat'eva, N. A. Danilov, S. V. Averkiev, M. V. Obrezkova, V. V. Lunin, E. N. Sobol', *J. Anal. Chem.* **2007**, *62*, 51.

[44] a) V. A. Parfenov, Y. D. Khesuani, S. V. Petrov, P. A. Karalkin, E. V. Koudan, E. K. Nezhurina, F. D. Pereira, A. A. Krokhmal, A. A. Gryadunova, E. A. Bulanova, I. V. Vakhrushev, I. I. Babichenko, V. Kasyanov, O. F. Petrov, M. M. Vasiliev, K. Brakke, S. I. Belousov, T. E. Grigoriev, E. O. Osidak, E. I. Rossiyskaya, L. B. Buravkova, O. D. Kononenko, U. Demirci, V. A. Mironov, *Sci. Adv.* **2020**, *6*, 4174; b) P. R. Baraniak, M. T. Cooke, R. Saeed, M. A. Kinney, K. M. Fridley, T. C. McDevitt, *J. Mech. Behav. Biomed. Mater.* **2012**, *11*, 63.

[45] B. P. Hung, J. N. Harvestine, A. M. Saiz, T. Gonzalez-Fernandez, D. E. Sahar, M. L. Weiss, J. K. Leach, *Biomaterials* **2019**, *189*, 1.

[46] C. E. Vorwald, S. S. Ho, J. Whitehead, J. K. Leach, *Methods Mol. Biol.* **2018**, *1758*, 139.